Sains Malaysiana 39(3)(2010): 479–484

Effect of Zirconium Substitution on the Phase Formation and Microstructure of $BaCeO_3$

(Kesan Penggantian Zirkonium ke Atas Pembentukan Fasa dan Mikrostruktur $BaCeO_3$)

N. OSMAN*, I.A. TALIB & H.A. HAMID

ABSTRACT

Polycrystalline compounds of $Ba(Ce_{1-x}Zr_x)_{0.95}Yb_{0.05}O_{2.975}$ ($0.20 \le x \le 0.40$) were prepared by the conventional solid state reaction method. All the samples exhibited the orthorhombic structure of $BaCeO_3$. The particle size and morphology of the powdered samples were found to change gradually with Zr content. The sample with x=0.40 showed more agglomerates of about 10.0 µm in size, and the particles constituting the agglomerates were smaller than 1.0 µm. For the polished and etched pelleted samples, only the x=0.20 sample showed clear grain shapes with sizes in the range of 1.0 to 3.0 µm. By increasing the Zr content to more than 20 mol%, the grain sizes became less pronounced and smaller. The deficiency of Ba that caused the formation of a Ce, Zr and Yb-rich sample was detected by energy dispersive X-ray measurement. Ba deficiency was attributed to the loss of BaO during the calcination and sintering processes.

Keywords: Cerate-zirconate; microstructure; oxides ceramic; phase formation

ABSTRAK

Polihablur sebatian polihablur $Ba(Ce_{1-x}Zr_x)_{0.95}Yb_{0.05}O_{2.975}$ ($0.20 \le x \le 0.40$) telah disediakan melalui kaedah tindak balas keadaan pepejal konvensional. Semua sampel menunjukkan struktur ortorombik bagi $BaCeO_3$. Saiz zarah dan morfologi serbuk sampel didapati berubah dengan kandungan Zr. Sampel dengan x=0.40 mempamerkan banyak aglomerat yang bersaiz lebih kurang 10.0 µm dan zarah-zarah yang membentuk aglomerat tersebut bersaiz lebih kecil daripada 1.0 µm. Untuk pelet yang digilap dan dipunarkan, hanya sampel x=0.20 menunjukkan bentuk butiran yang jelas dengan saiz antara 1.0 hingga 3.0 µm. Dengan penambahan kandungan Zr lebih daripada 20 %mol, saiz butiran menjadi kurang jelas dan semakin mengecil. Kekurangan unsur Ba yang dikesan menggunakan spektroskopi sebaran tenaga sinar-X telah menyebabkan pembentukan fasa yang kaya dengan Ce, Zr and Yb di dalam sampel kajian. Kekurangan unsur Ba ini adalah disebabkan oleh kehilangan BaO semasa proses pengkalsinan dan persinteran.

Kata kunci: Mikrostruktur; pembentukan fasa; serat-zirkonat; seramik oksida

INTRODUCTION

Perovskites based on cerate and zirconate become protonic conductors when doped with trivalent or divalent cations (Iwahara 1992). The general formula for these materials is $AB_{1-x}M_xO_{3-\alpha}$, where $\alpha = \frac{x}{2}$. Cerates show higher conductivity than zirconates, but in terms of mechanical and chemical stability, doped zirconates are more stable than cerates (Yajima et al. 1992). Considering the advantages of each material, several studies on zirconium-substituted barium cerates have been reported (Azad & Irvine 2007; Bae et al. 2001; Katahira et al. 2000; Matzke & Cappadonia 1996).

It is well known that microstructure is one of the most important features controlling the mechanical properties and surface behavior of ceramic materials. However, works on the microstructure and phase formation of the $Ba(Ce_{1-x}Zr_x)_{0.95}Yb_{0.05}O_{2.975}$ system have not been widely reported. Therefore, the present work was conducted to gain further insight into the effects of chemical-physical inhomogeneities and minor impurities on the microstructure development of cerate-zirconate ceramics during the sintering process.

EXPERIMENTAL METHOD

Appropriate ratios of $BaCO_3$ (Aldrich), CeO_2 (Aldrich), ZrO_2 (Acros) and Yb_2O_3 (Aldrich) were manually mixed and ground in an agate mortar with pestle, then calcined at 1700 °C for 10 in air. The reaction product was again ground for 30 min and stored in a desiccator prior to pressing. The powders were pressed with a pressure of 5-6 tons for 5-10 min into pellets of 13 mm diameter and 1 mm thickness. The pellets were sintered at 1650 °C for 10 hours in air. The density of each pellet was determined using a geometrical method involving weighing and measuring the dimensions of the pellet. The surface of

each pellet was polished with 6 μm and subsequently 1 μm polishing cloths. All the polished samples were then etched in HNO_3 for 30 s.

X-ray diffraction (XRD) was used to obtain the crystal structure of the calcined powders. XRD measurements were carried out at room temperature using a Bruker AXS D8 (Cu-K_α, λ=1.5406 Å) X-ray diffractometer from 20° to 80° with scanning rate of 0.02 s^{-1}.

The homogeneity and particle size of the calcined powders were determined by LEO scanning electron microscope (SEM), model Supra 50 VP. A sample in powder form was coated with gold using the Polaron (Fisons) SC515 Sputter Coater. The microstructures and chemical compositions of the polished pellets were obtained using a field emission scanning electron microscope (FESEM), model LEO 1525, and an energy dispersive X-ray (EDX), model Oxford INCA version 17a, respectively. The samples were mounted in a sample holder prepared by a cold molded technique using a mixture of resin and hardener. The mounted sample was gold coated by the SC7640 Sputter Coater (Polaron).

Results and Discussion

Figure 1 shows the X-ray diffractogram of the samples calcined at 1700 °C for 10 h All the existing peaks correspond to the perovskite structure of 'pure' $BaCeO_3$ (Joint Committee of Powder Diffraction Standards (JCPDS) card no. 22-0074). As the Zr content increased, the peak positions were gradually shifted to higher angles of 2θ (Figure 1), indicating that the unit cell volume of the samples decreased. The same observation was also reported by Ryu and Haile (1999) for the sample $BaCe_{0.9-x}Zr_xM_{0.1}O_{3-\alpha}$ (M=Gd, Nd). Table 1 shows the lattice parameters and unit cell volume of the $Ba(Ce_{1-x}Zr_x)_{0.95}Yb_{0.05}O_{2.975}$ samples. For comparison, we also included the values of the lattice parameters and unit cell volume for 'pure' $BaCeO_3$. The contraction of the unit cell volume of the samples compared to the 'pure' $BaCeO_3$ can be used to suggest a complete substitution of Zr and Yb cations at Ce sites, as reported in our previous work (Osman 2006). There were no new peaks noticeable in the spectra, indicating that no other phases were present in the sample.

Figure 2 shows the morphology of the calcined powder samples. Most of the particles are almost spherical in shape and have sizes within 0.5 to 2.0 μm. The particle size and morphology of the powder samples seem to gradually change with Zr content. By increasing the Zr content, the samples tend to form agglomerates. The sample with x=0.40 showed a significant number of agglomerates. The agglomerates were approximately 10.0 μm in size, while the sizes of the particles constituting these agglomerates were smaller than 1.0 μm. The presence of more agglomerates would lead to non-homogeneous particle size, consequently producing a poor sinterability, as shown by the sample with higher Zr content. The sample with x=0.40 exhibited a relative density of about 66% of the theoretical density, while other samples were in the range of 80% to 90%.

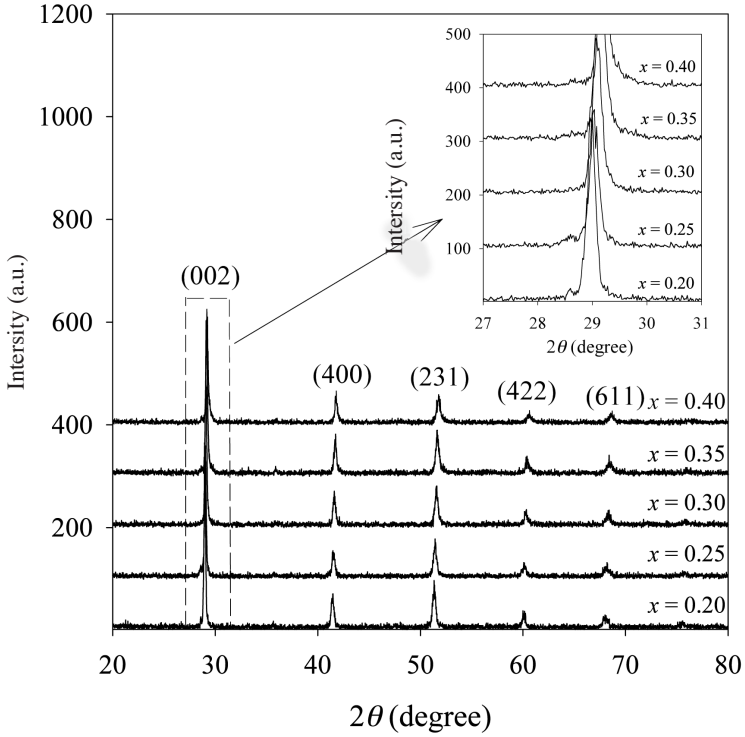

FIGURE 1. XRD patterns for $Ba(Ce_{1-x}Zr_x)_{0.95}Yb_{0.05}O_{2.975}$ samples calcined at 1700 °C. (*Insert* is a graph for the (002) plane showing that the peak position is gradually shifted to a higher angle as the Zr content increases)

TABLE 1. Lattice parameters and unit cell volume of $Ba(Ce_{1-x}Zr_x)_{0.95}Yb_{0.05}O_{2.975}$

Sample	a (nm)	b (nm)	c (nm)	V (nm^3)
$BaCeO_3$ (JCPDS card no. 22-0074)	0.8779	0.6214	0.6236	0.3402
x=0.20	0.8711	0.6157	0.6166	0.3307
x=0.25	0.8704	0.6143	0.6148	0.3287
x=0.30	0.8670	0.6142	0.6129	0.3264
x=0.35	0.8656	0.6141	0.6116	0.3251
x=0.40	0.8636	0.6102	0.6110	0.3220

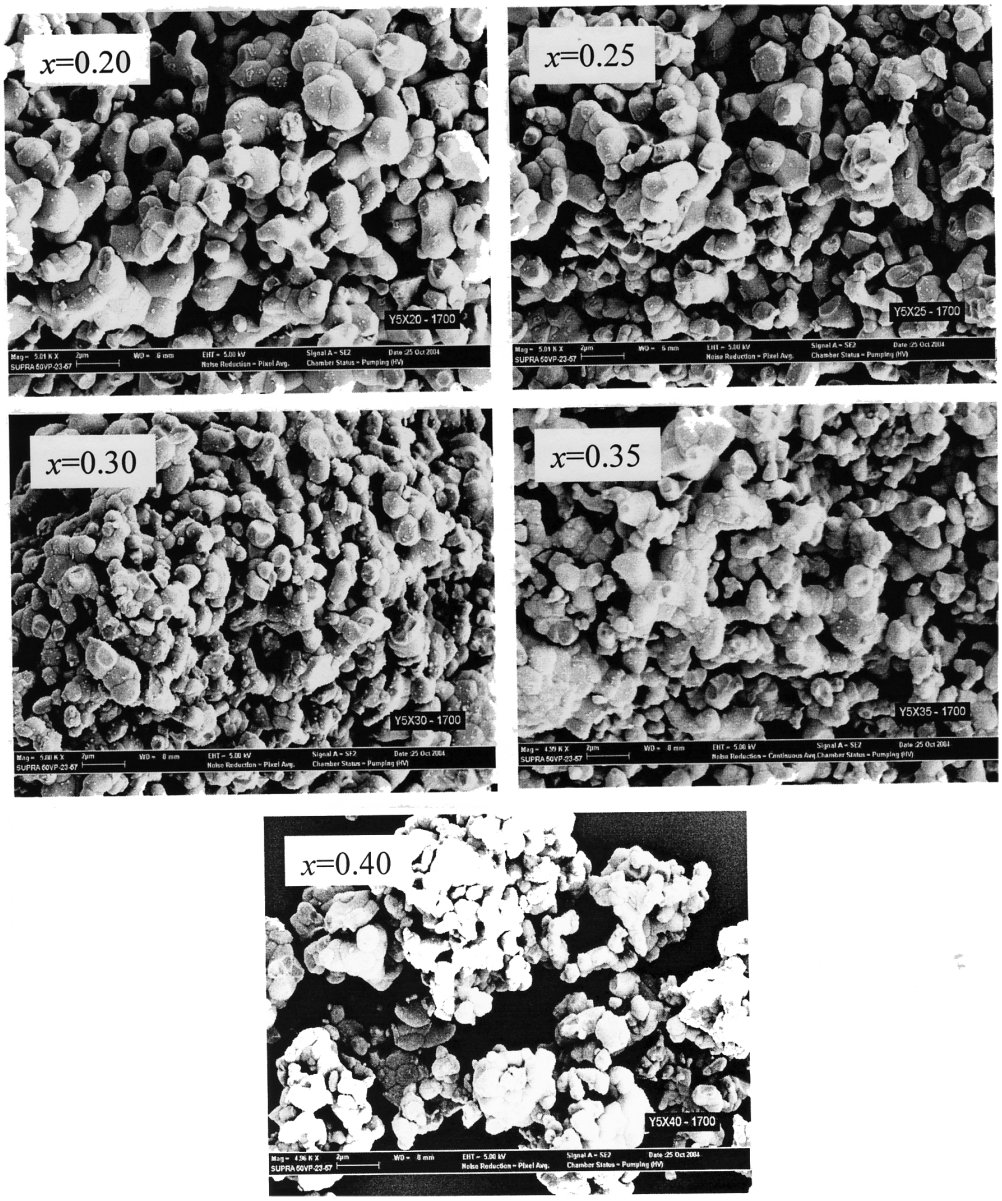

FIGURE 2. SEM images of the calcined powder for the $Ba(Ce_{1-x}Zr_x)_{0.95}Yb_{0.05}O_{2.975}$ samples at various concentrations of Zr

TABLE 2. Elemental compositions of $Ba(Ce_{1-x}Zr_x)_{0.95}Yb_{0.05}O_{2.975}$, x=0.20 during spot analysis

Elements	Weight percent			
	Spectrum 11	Spectrum 12	Spectrum 13	Spectrum 14
C	1.28	1.17	1.53	1.71
O	15.70	14.14	14.44	13.52
Zr	8.49	13.81	9.21	13.21
Ba	1.42	39.12	4.38	24.25
Ce	59.02	28.28	56.94	39.92
Yb	14.09	3.48	13.50	7.40

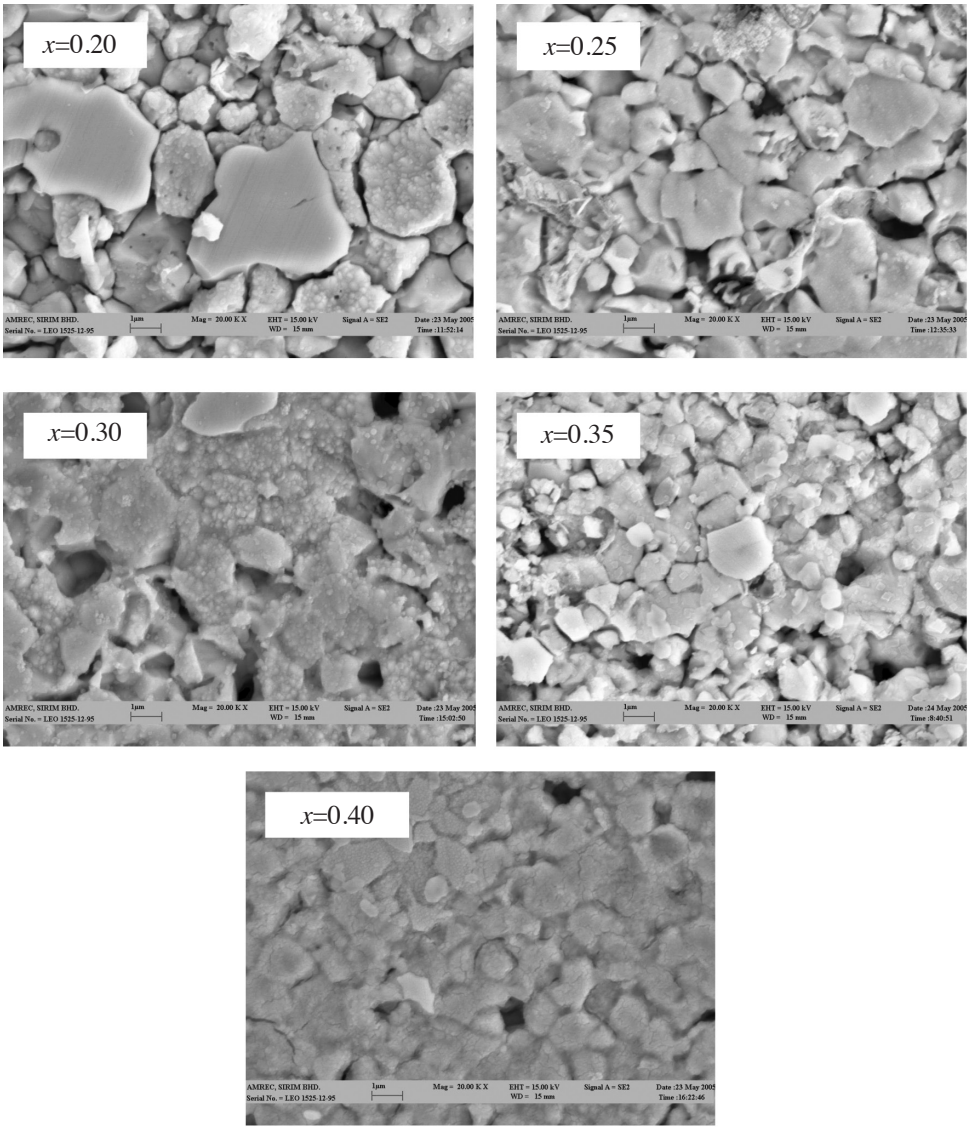

FIGURE 3. SEM images of the sintered, polished and etched pellets of $Ba(Ce_{1-x}Zr_x)_{0.95}Yb_{0.05}O_{2.975}$ at various concentrations of Zr (magnification ≈ 20,000x)

The effect of Zr concentration on the microstructure of polished and etched pellets is shown in Figure 3. Clear grain shapes can only be seen for the sample with x=0.20. This sample showed uniform grain size distribution, and its grain sizes were in the range of 1.0 to 3.0 μm. However, by increasing the Zr content, the formation of grains became less pronounced and of generally smaller grain size. The grains of samples with x=0.25 and x=0.35 have sizes in the range of 0.5 to 2.0 μm. The lack of clear grain boundaries in the x=0.30 sample makes it difficult to estimate the size of the grains for this sample. The grains constituting the agglomerates of the sample with x=0.40 have the smallest size (0.5–1.0 μm) compared to the others.

Figure 4 shows the SEM for the x=0.20 sample of four spots where the EDX analyses were obtained. The elemental composition of each spot is summarized in Table 2. The results revealed that the sample tends to form Ce, Zr and Yb clusters due to the Ba-deficit. The deficiency of Ba was suspected due to the evaporation of BaO during high temperature calcination and sintering processes. Snijkers et al. (2004a) also reported that the Y:ZrO_2-phase formed at the surface of the $BaZr_{0.9}Y_{0.1}O_{3-\delta}$ pellet was due to the loss of BaO during sintering of the sample at 1700 °C. They used an X-ray beam at a low angle (0.5°) during XRD measurement to detect the phase. In addition, they also determined BaO losses during high temperature processing for $Ba_xHf_{0.9}Y_{0.1}O_{3-\alpha}$ powder by WD-XRF using pre-calibrated spectral lines (Snijkers et al. 2004b). Ryu and Haile (1999) also reported that CeO_2 precipitates on the surface of $BaCe_{0.9-x}Zr_xNd_{0.1}O_{3-\delta}$ and $BaCe_{0.9-x}Zr_xGd_{0.1}O_{3-\delta}$ samples due to the evaporation of BaO, as determined via both x-ray examination and visual inspection.

As the Zr content increased, the amount of Zr-rich clusters became relatively higher than the amounts of Ce and Yb clusters. Thus, we believe that the presence of agglomerates and the formation of unclear grain boundaries were caused by the increase of Zr-rich phases. All the clusters were distributed randomly in the samples. As a result, the compositions of the samples deviated slightly from the prepared stoichiomteric ratio, giving rise to the fluctuations of chemical composition. In this study, the amount of Ba deficit was detected in the EDX analysis even though the XRD patterns show a single-phase compound corresponding to $BaCeO_3$. This result is in line with literature discussed by Haile et al. (2001) in which doped perovskite, depending on the dopant ion, remained single phase even under highly non-stoichiometric conditions (4-10 mol% Ba deficient).

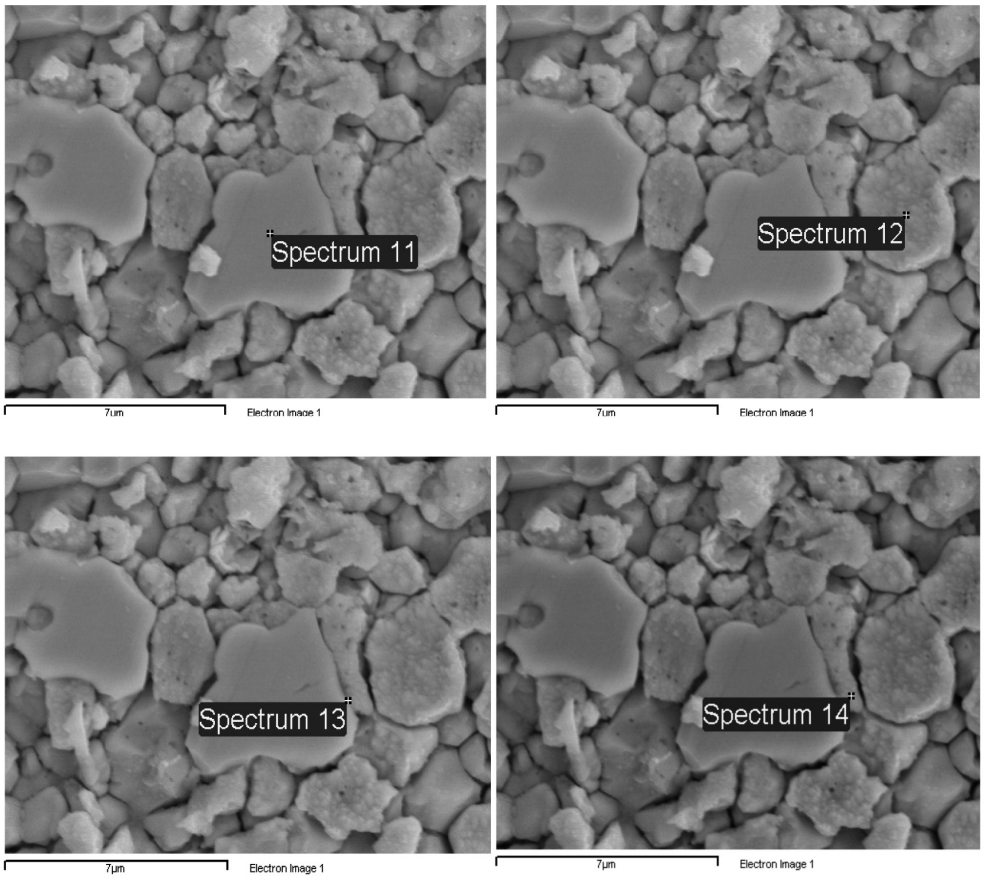

FIGURE 4. SEM images of $Ba(Ce_{1-x}Zr_x)_{0.95}Yb_{0.05}O_{2.975}$, x=0.20, for EDX analysis (spectra 11 to 14 are indicators for the spot analysis)

CONCLUSION

A calcination temperature of 1700 °C was needed to complete the decomposition of carbonate and oxide precursors to yield a pure perovskite-like phase of barium cerate with orthorhombic structure. Scanning electron micrographs revealed that the particle size was in the sub-micron size range (0.5 to 2.0 μm). As Zr content increased, the formation of grains became less pronounced and of generally smaller grain size. Ba deficiency occurred in bulk materials sintered at high temperatures, generating non-stoichiometric samples.

ACKNOWLEDGEMENTS

The authors wish to thank Universiti Teknologi MARA for supporting this project under IRDC grant no.600-IRDC/ST.5/3/637 and the School of Material & Mineral Resource, Engineering Campus, Universiti Sains Malaysia and the Advanced Materials Research Centre (AMREC) in Kulim, Kedah, Malaysia for the support.

REFERENCES

Azad, A.K. & Irvine, J.T.S. 2007. Synthesis, chemical stability and proton conductivity of the perovskites $Ba(Ce,Zr)_{1-x}Sc_xO_{3-\delta}$. *Solid State Ionics* 178: 635-640.

Bae, J.S., Choo, W.K. & Lee, C.H. 2001. The crystal structure of $Ba(Ce_{0.8}Zr_{0.2})O_3$. *Journal of the European Ceramic Society* 21: 1779-1782.

Haile, S.M., Staneff, G. & Ryu, K.H. 2001. Non-stoichiometry, grain boundary transport and chemical stability of proton conducting perovskites. *Journal of Materials Science* 36: 1149-1160.

Iwahara, H. 1992. Oxide-ionic and protonic conductors based on perovskite-type oxides and their possible applications. *Solid State Ionics* 52: 99-104.

Katahira, K., Kohchi, Y., Shimura, T. & Iwahara, H. 2000. Protonic conduction in Zr-substituted $BaCeO_3$. *Solid State Ionics* 138: 91-98.

Matzke, T. & Cappadonia, M. 1996. Proton conductive perovskite solid solutions with enhanced mechanical stability. *Solid State Ionics* 86-88: 659-663.

Osman, N., Jani, A.M. & Talib, I.A. 2006. Synthesis of Yb-doped $Ba(Ce,Zr)O_3$ ceramic powders by sol-gel method. *Ionics* 12: 379-384.

Ryu, K.H. & Haile, S.M. 1999. Chemical stability and proton conductivity of doped $BaCeO_3$-$BaZrO_3$ solid solutions. *Solid State Ionics* 125: 355-367.

Snijkers, F.M.M., Buekenhoudt, A., Cooymans, J. & Luyten, J.J. 2004a Proton conductivity and phase composition in $BaZr_{0.9}Y_{0.1}O_{3-\alpha}$. *Scripta Materialia* 50: 655-659.

Snijkers, F.M.M., Buekenhoudt, A., Luyten, J.J., Cooymans J. & Mertens, M. 2004b. Proton conductivity in perovskite type yttrium doped barium hafnate. *Scripta Materialia* 51: 1129- 1134.

Yajima, T., Suzuki, H., Yogo, T. & Iwahara, H. 1992. Protonic conduction in $SrZrO_3$ based oxides. *Solid State Ionics* 51: 101-107.

N Osman* & H.A. Hamid
Faculty of Applied Sciences
Universiti Teknologi MARA
02600 Arau
Perlis, Malaysia

I. A. Talib
Faculty of Science & Technology
Universiti Kebangsaan Malaysia
43600 Bangi
Selangor, Malaysia

*Corresponding author; email: fisha@perlis.uitm.edu.my

Received: 22 June 2009
Accepted: 10 September 2009